17th World Conference on Earthquake Engineering, 17WCEE
Sendai, Japan - September 13th to 18th 2020

LANDSLIDE RUNOUTS OBSERVED IN THE 2018 HOKKAIDO EASTERN IBURI EARTHQUAKE

K. Konagai[(1)], A. M. Nakata[(2)]

[(1)] *Professor Emeritus, University of Tokyo, kaz3776k@gmail.com*
[(2)] *Researcher, International Consortium on Landslides, amnakata@gmail.com*

Abstract

The major impact of the Mw 6.6 September 6th, 2018 Hokkaido Eastern Iburi Earthquake was obviously in the form of geotechnical failures. The intense tremor triggered more than 3,300 landslides confirmed over an area of about 20 km × 20 km near Atsuma Town, wiping out homes sparsely distributed along bases of hills [1, 2]. Around 80% of 41 victims were confirmed dead of suffocation. This calamity has left a big question about how far out a landslide mass can travel. Since the majority of more than 3,300 landslides in the epicentral area were shallow and planar masses of volcanic ash and pumice, and these masses have deposited over extensive flat rice fields sometimes dotted with farmhouses, a discussion is made herein about common geometric features of these landslide masses, which are expected to provide a clue as to possible runout distances of these landslide masses. The noteworthy common factures of almost all landslides in the epicentral area of this earthquake are that (1) root systems that can help trees "grab onto" soil and keep it clumped together hardly penetrated through the pumice/ volcanic ash drape and stayed above the slip surfaces, and that (2) almost an entire body of each landslide mass deposited over a flat land with little fraction of the mass remaining on the slope. Given these common features, dimensions of landslide masses that have deposited over flat rice fields have been examined. A multiple linear regression analysis for the relationship among the measured dimensions of these landslide masses has given us both the average values of mobilized frictional coefficients μ_1 (about 0.17) on the slip surfaces and μ_2 (about 0.36) on the flat rice fields. However, the value of μ_1 for a smaller and gentler slope, which might have been wetter than the others, could have been even smaller than this average value. The observed geometric features of these landslide masses have a strong resemblance to those on hill slopes of Hachinohe area draped with volcanic products; those masses were detached in the May 16th, 1967 Off the Coast of Tokachi Earthquake. The runout distances of those landslide masses are also discussed comparing them with the ones in the 2018 Hokkaido Earthquake.

Keywords: 2018 Hokkaido Eastern Iburi Earthquake; Landslide runout; drapes of volcanic products

1. Introduction

A Mw 6.6 earthquake rocked the northern Japanese island of Hokkaido on September 6, 2018 at 3:08 a.m. JST. The Japan Meteorological Agency (JMA) has given it an official name “the 2018 Hokkaido Eastern Iburi Earthquake” (2018 Hokkaido Earthquake, hereafter). The earthquake occurred just one day after the edge of a powerful typhoon Jebi left traces of destruction in the region. The major impact of this earthquake was obviously in the form of geotechnical failures [1, 2]. The intense tremor triggered more than 3,300 landslides confirmed over an area of about 20 km × 20 km near Atsuma Town [3], wiping out homes sparsely distributed along bases of hills. Around 80% of 41 victims were confirmed dead of suffocation [4].

This calamity has left a big question about how far out a landslide mass can travel. Since the majority of more than 3,300 landslides in the epicentral area were shallow and planar masses of volcanic ash and pumice and they have deposited over extensive flat rice fields sometimes dotted with farmhouses, a discussion is made herein about common geometric features of these landslide masses; which are expected to provide a clue as to possible runout distances of these landslide masses.

The geometric features of these landslide masses have a strong resemblance to those on hill slopes of Hachinohe area draped with volcanic products; those masses were detached in the May 16th, 1967 Off the Coast of Tokachi Earthquake (1968 Tokachi Earthquake, hereafter). The runout distances of those landslide masses are also discussed comparing them with the ones in the 2018 Hokkaido Earthquake.

2. Dimensions of landslide masses and runouts

Eruptions of major volcanoes such as Shikotsu (about 40,000 years ago), Tarumae (about 20,000 years ago) and Eniwa (about 9,000 years ago) have left layers of volcanic matters such as pumice draping the hilly landscape with sediments deposited on top later [5]. These pumice-rich layers seem to have collapsed in the intense shake and have caused the multiple landslides, which all look similar with each other in terms of color of the exposed bare earths, uprooted trees densely accumulated near the distal ends of landslide masses, etc. The noteworthy common features of these landslides are that (1) root systems that can help trees "grab onto" soil and keep it clumped together hardly penetrated through the pumice/ volcanic ash drape and stayed above the slip surfaces, and that (2) almost an entire body of each landslide mass has left the slope with little fraction of its mass remaining on the slope.

Given the abovementioned features of the multiple landslides, we focus exclusively on independent landslide masses that traveled over flat rice fields. Sometimes, these masses that spread over the flatland touch side by side with each other. However, as long as their interactions are not significant, we take them into targets of the examination just to assure substantial statistical significance.

A landslide mass with its initial length L_1 and cross-sectional area A_1 is assumed to have been decelerated as it traveled over a flat land and stopped completely with its final length L_2 and cross-sectional area A_2 immediately when the whole mass left the slope L_1 (Fig. 1).

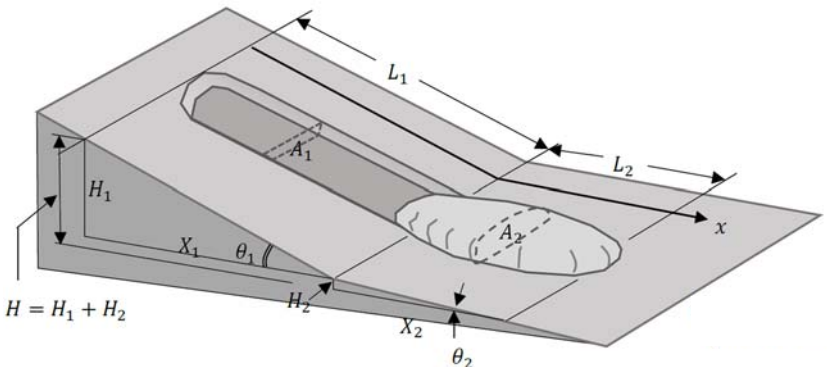

Fig. 1 – Schematic view of a planar landslide mass [1, 2]

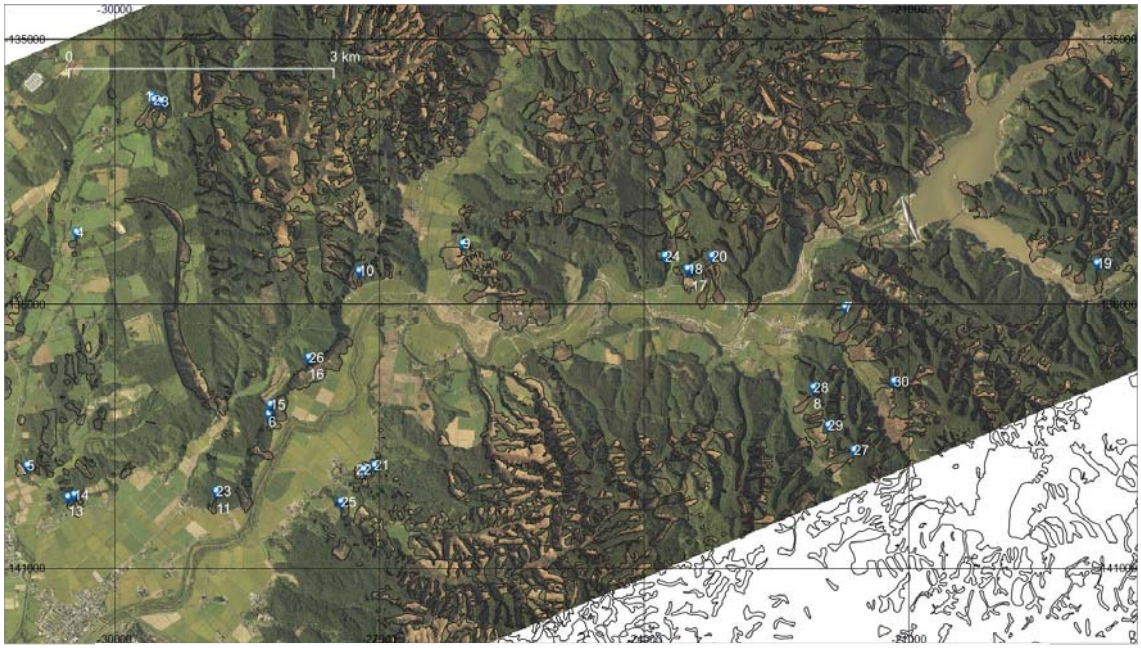

Fig. 2 – Near Atsuma Town, 30 landslides dimensions were measured. [2]
(Aerial photo from the Geospatial Information Authority of Japan)

The variations in A_1 and A_2 along the direction of the dip (x) are assumed to be substantially small and fluctuate little around their average values $\bar{A}_1$ and $\bar{A}_2$. Since the landslide mass does not change its mass M, $\rho_i \bar{A}_i L_i = M$ is kept constant where ρ_i, $\bar{A}_i$, and L_i are respectively density, average cross-sectional area and length of the landslide mass with $i =$ either 1 or 2 for the initial or the final stage of sliding. Total 30 landslide masses shown with blue place-marks in Fig. 2 were examined, and the dimensions of these landslide masses are listed in Table 1.

The work W_1 used up through friction exerted upon the sliding surface L_1 is given by:

$$W_1 = \int_0^{L_1} \rho_1 g A_1 (L_1 - x) \cos\theta_1 \, \mu_1 dx$$
$$= \rho_1 g \bar{A}_1 L_1 \cos\theta_1 \, \mu_1 \frac{L_1}{2} = Mg \cos\theta_1 \, \mu_1 \frac{L_1}{2} \quad (1)$$

where, g is the gravitational acceleration, $\cos\theta_1$ is the cosine of the average dip of the slope L_1, and is given by :

$$\cos\theta_1 = \frac{X_1}{L_1} \quad (1a)$$

μ_1 is the mobilized frictional coefficient on the sliding surface L_1, which is assumed to be uniform over the whole stretch of the slope. Likewise, the work W_2 used through friction exerted upon the depositional area L_2 is given by:

$$W_2 = \int_0^{L_2} \rho_2 g A_2 x \cos\theta_2 \, \mu_2 dx$$
$$= \rho_2 g \bar{A}_2 L_1 \cos\theta_2 \, \mu_2 \frac{L_2}{2} = Mg \cos\theta_2 \, \mu_2 \frac{L_2}{2} \quad (2)$$

where, μ_2 is the frictional coefficient on the depositional area L_2, and $\cos\theta_2$ is given by:

$$\cos\theta_2 = \frac{X_2}{L_2} \quad (2a)$$

Table 1 – Dimensions of 30 landslide masses shown in Fig. 2 [2]

ID	Location of top scar		L_1 (m)	L_2 (m)	H_1 (m)	H_2 (m)	H (m) $(H_1 + H_2)$	X_1(m)	X_2(m)
	East Longitude (degree)	North Latitude (degree)							
1	141.8885	42.7776	205.3	108.6	72.1	13.3	85.3	192.2	107.8
2	141.8888	42.7772	156.3	106.5	64.3	2.3	66.6	142.5	106.5
3	141.8898	42.7770	120.7	101.4	40.8	8.8	49.5	113.6	101.0
4	141.8781	42.7636	87.9	14.6	12.3	0.2	12.5	87.1	14.6
5	141.8714	42.7398	70.5	46.5	24.9	-0.1	24.9	65.9	46.5
6	141.9048	42.7451	78.4	93.3	30.8	2.8	33.6	72.0	93.2
7	141.9846	42.7564	159.7	106.3	56.2	8.2	64.5	149.4	106.0
8	141.9803	42.7480	150.4	165.4	69.8	8.7	78.5	133.2	165.1
9	141.9316	42.7627	134.0	121.1	48.9	4.8	53.7	124.8	121.0
10	141.9172	42.7599	71.7	27.3	31.3	4.6	35.9	64.5	26.9
11	141.8976	42.7371	96.2	68.6	34.6	1.5	36.2	89.7	68.6
12	141.8743	42.7149	42.6	11.9	9.7	0.1	9.8	41.5	11.9
13	141.8771	42.7366	105.6	37.0	13.4	0.1	13.5	104.8	37.0
14	141.8779	42.7368	101.1	64.7	14.6	0.2	14.8	100.0	64.7
15	141.9050	42.7461	77.9	131.3	38.7	3.1	41.8	67.6	131.3
16	141.9104	42.7509	115.1	90.2	42.1	1.8	43.8	107.1	90.2
17	141.9633	42.7601	113.6	77.6	65.2	4.4	69.6	93.0	77.5
18	141.9627	42.7602	106.8	68.7	63.6	4.2	67.8	85.8	68.6
19	142.0194	42.7609	144.5	125.4	79.8	14.0	93.8	120.4	124.6
20	141.9661	42.7615	308.8	163.3	93.1	3.5	96.6	294.5	163.3
21	141.9195	42.7400	96.8	46.3	26.9	0.4	27.3	93.0	46.3
22	141.9180	42.7395	106.1	56.3	31.2	0.7	31.8	101.4	56.3
23	141.8976	42.7372	83.7	96.3	39.3	3.7	43.0	73.9	96.3
24	141.9596	42.7614	49.2	32.0	27.1	2.1	29.2	41.0	31.9
25	141.9149	42.7362	65.3	41.8	23.7	-0.1	23.5	60.8	41.8
26	141.9104	42.7509	116.1	85.2	42.8	1.0	43.8	107.9	85.2
27	141.9858	42.7417	189.7	159.8	86.6	4.0	90.6	168.8	159.8
28	141.9802	42.7480	152.0	159.3	71.2	8.3	79.5	134.4	159.1
29	141.9822	42.7442	110.9	85.9	58.3	3.7	62.0	94.4	85.8
30	141.9914	42.7487	99.0	141.5	54.8	4.3	59.0	82.5	141.5

In addition to the above, there is an energy dissipation process in the interior of the deforming landslide mass to be sure, but this energy dissipation is assumed to be less significant than W_1 and W_2. Thus, the summation of these works is considered to be nearly equal to the initial potential energy of the landslide mass given by:

$$E_p = \frac{MgH}{2} = \frac{Mg(H_1 + H_2)}{2} \tag{3}$$

Equating Equation (3) with Equation (1) + Equation (2), one obtains:

$$H \cong \cos\theta_1 \, \mu_1 L_1 + \cos\theta_2 \, \mu_2 L_2 = \mu_1 X_1 + \mu_2 X_2 \tag{4}$$

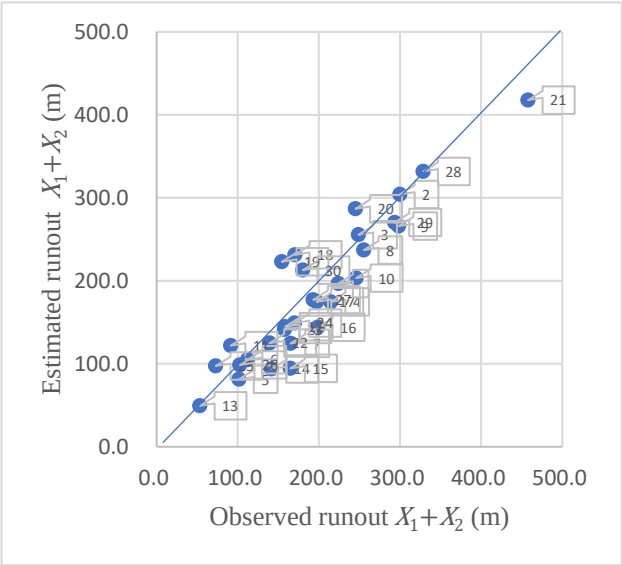

Fig. 3 – Comparison of the observed and estimated runouts $X_1 + X_2$ values. [2]

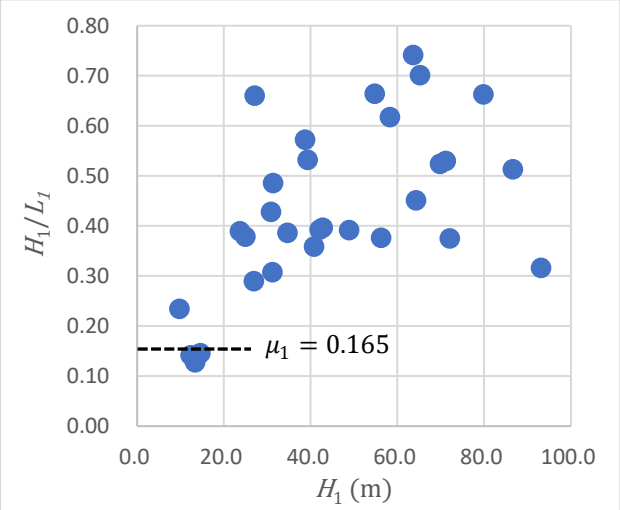

Fig. 4 – Slope inclinations H_1/L_1 for different relative heights of top scars H_1. [2]

If the variations in μ_1 and μ_2 are substantially small and follow normal distributions, a multiple linear regression analysis for the relationship between the dependent variable H and two independent variables X_1 and X_2 with its intercept set at zero can give us the overall picture of the mobilized frictional coefficients.

For the 30 landslides (28 degrees of freedom) listed in Table 1, the average values of $\mu_1 = 0.165$ and $\mu_2 = 0.36$ were obtained with the standard errors of $\sigma_{\mu_1} = 0.058$ and $\sigma_{\mu_2} = 0.069$, respectively, and the coefficient of determination, $R^2 = 0.94$. Thus, runout distances $X_1 + X_2$ can be predicted using the following equation:

$$X_1 + X_2 \cong \frac{H}{\mu_2} + \left(1 - \frac{\mu_1}{\mu_2}\right) X_1 = 2.8H + 0.54X_1 \cong 2.8H_1 + 0.54X_1 \quad (5)$$

Fig. 3 compares the observed and estimated runout distances $X_1 + X_2$ for the examined 30 landslides. Though Equation (5) helps understand the overall image of devastation, it is perhaps premature to discuss each detail only with the average values of μ_1 and μ_2 obtained from the 30 landslides, because there were no small number of slopes that have slipped even with their inclinations smaller than the average value of $\mu_1 = 0.165$. It must be remembered that many landslides including these gentle slopes are inevitably on the unsafe (right) side of the prediction line (Equation (5)) drawn on Fig. 3.

Fig. 4 plots slope inclinations H_1/L_1 of the chosen 30 landslides against the heights of their top scars H_1. As a whole, the smaller the H_1 values are, the smaller are the inclinations H_1/L_1, and three slopes are found below the $H_1/L_1 = 0.165$ line in this figure. In the authors' previous report [2], μ_1 was examined using a small landslide on a very gentle slope shown in Fig. 5 with $H_1 \cong 20$ m and $H_1/L_1 \cong 0.2$. This planar landslide mass, after sliding on this gentle slope, hit the opposite wall of the shallow valley and formed a transverse bulge as illustrated in Fig. 6. This bulge was assumed to have developed where wedges of passive soil failure formed one after another at the boundary between the toe part pressed against the opposite valley wall and the slowing tail part with the uniform thickness t as illustrated in Fig. 6. This tail part was gradually shortening until its final length of L_{final} was reached. Given this assumption, μ_1 was obtained to be 0.05 as much.

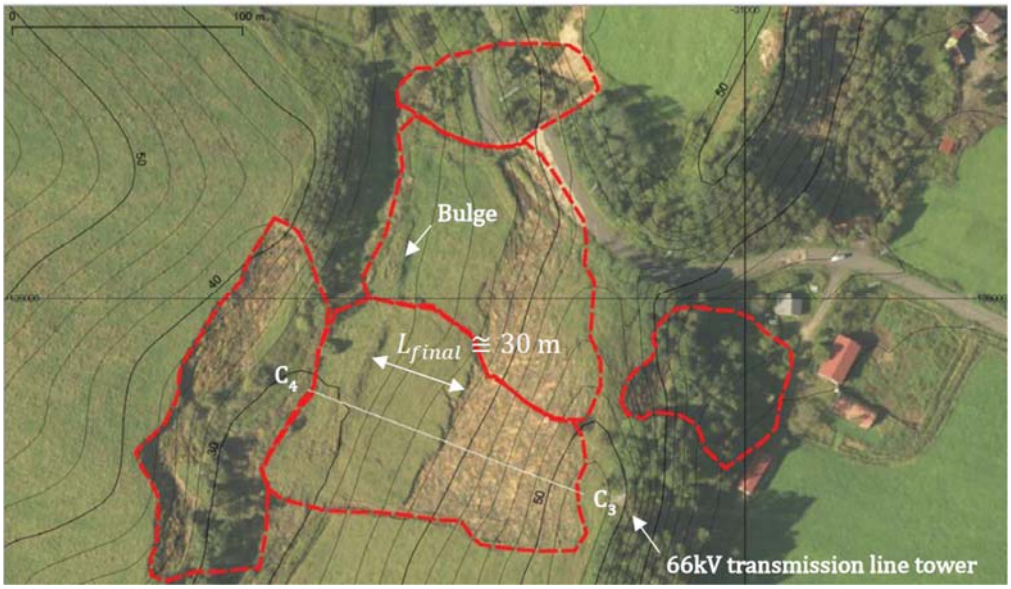

Fig. 5 – Coherent landslide mass compressed against the other side wall of valley [1, 2]

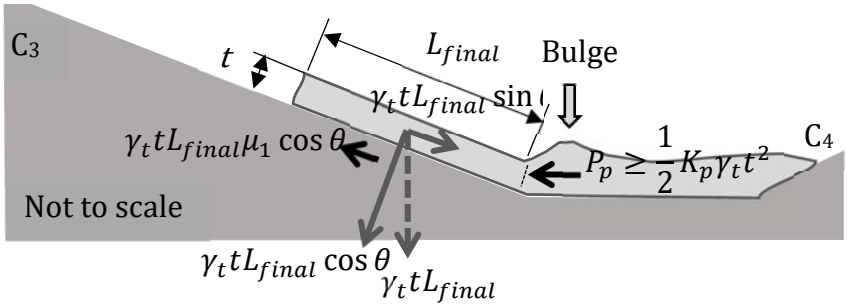

Fig. 6 – Cross-section of landslide mass that has stopped moving being compressed against the other side wall of valley[1, 2] (not to scale):

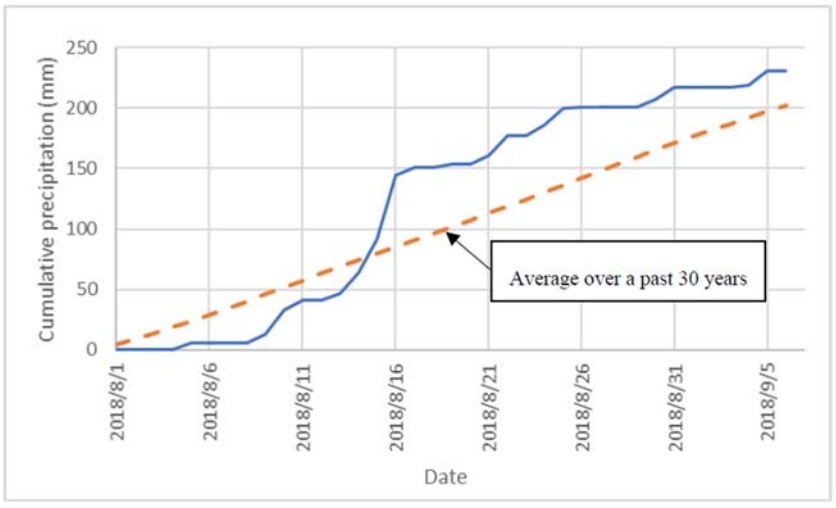

Fig. 7 – Cumulative precipitation at Atsuma station of Automated Meteorological Data Acquisition System (AMeDAS) at N42.730, E141.888, for the period from August 1 to Sept. 6, 2018 [2]

(Data from the Japan Meteorological Agency[6])

The gentler and the smaller slopes are, the wetter they may have been, because the greater parts of slip surfaces formed in the small and gentle slopes could have been well beneath the seepage lines, given the cumulative precipitation in the epicentral area (at Atsuma station of Automated Meteorological Data Acquisition System (AMeDAS)) for the period from August 1 to September 6, 2018 (the date of the earthquake), exceeding the average for the same period over a past 30 years (1981 - 2010) by about 50 mm (Fig. 7).

3. Strong resemblance to a past case history

The observed geometric features of these landslide masses have a striking resemblance to those on hill slopes in Hachinohe, Aomori Prefecture, draped with pumice-rich volcanic products from an explosive eruption of Mt. Towada (about 13,000 years ago). These multiple landslides were caused by the Tokachi Earthquake of 1968. As we saw in the case of the 2018 Hokkaido Earthquake, many victims (33 of the total 46) in this earthquake were also confirmed dead of suffocation [7]. The earthquake occurred on May 16 at 0:49 UTC (09:49 local time) in the area offshore Aomori and Hokkaido with its moment magnitude put at M_w8.3. This earthquake was preceded by a heavy rain due to a trough of low pressure [7]. Fig. 8 is the map of 3-days (May 13-15, 1968) rainfall accumulation in Aomori Prefecture [7, 8]. It is noted in this figure that the 3-days cumulative rainfall of about 200 mm in the area of the multiple landslides (dashed-line box) was eventually the heaviest in this prefecture. Fig. 9 (a) and (b) show an illustration in Reference [9] and an aerial photo (TO6810Y [10]) of triple landslides at Nakazutesu, Gonohe Town, respectively; they look almost exactly like the ones in Atsuma, Hokkaido (Fig. 9 (c)). Locations of 6 landslides were identified through aerial photographic image interpretation and pinpointed with blue placemarks on the digital terrain model (Fig. 10) to extract their slope dimensions H_1, H_2, X_1 and X_2 (see Fig. 2); these dimensions were summarized in Table 2. One cannot draw any statistically significant result only with the six examples. Therefore, the parameters in Table 2 were substituted in Equation (5) to compare the actual runout distances of these landslide masses with the estimated ones assuming that the masses have the same physical features as those in the multiple landslides area in Hokkaido (Fig. 11). The slope of 0.9155 (< 1.0) of the trendline passing through the origin and these six points in Fig. 11 shows that the actual runout distances are in general slightly longer than the estimated distances, and the coefficient of determination, $R^2 = 0.9728$, of this trendline implies that there is a striking resemblance between the Hachinohe and Hokkaido multiple landslide areas in terms of not only their appearances but also their runout distances. Kawakami et al. [8] identified slip surfaces in six borehole logs from different landslide locations (Fig. 12). The identified slip surfaces are all similar lying about 2 m underground with less-dispersed dry density values ranging from 0.82 to 0.99 showing porous and crushable nature of the pumice-rich soil.

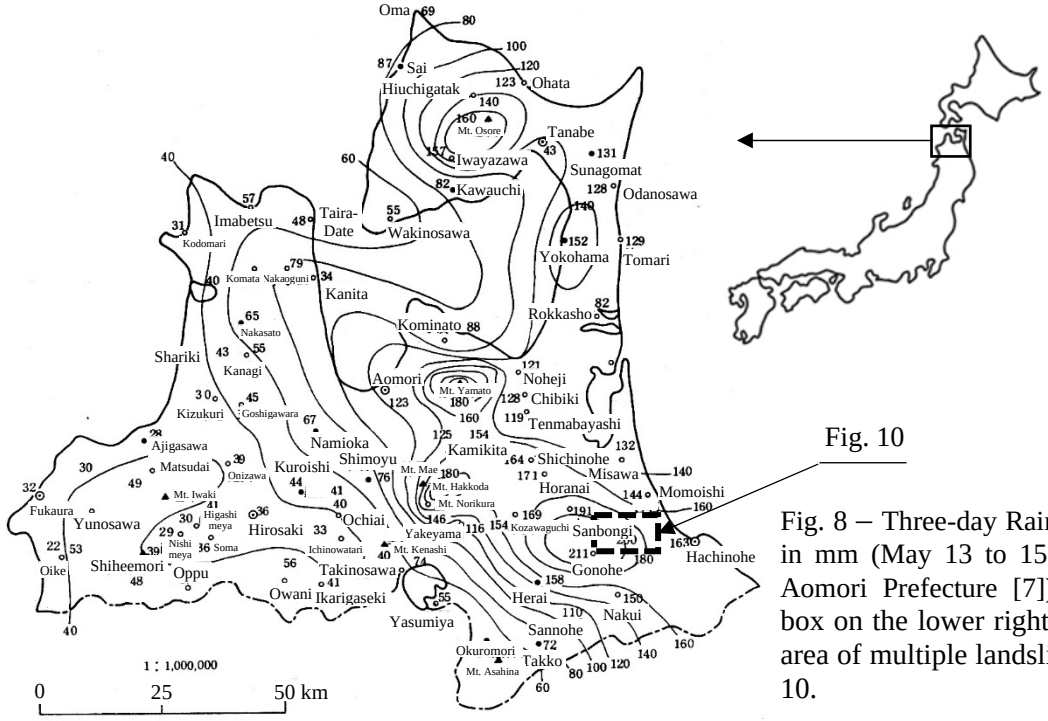

Fig. 10

Fig. 8 – Three-day Rainfall Accumulation in mm (May 13 to 15, 1968, Data from Aomori Prefecture [7]). A dashed-line box on the lower right of the map is the area of multiple landslides shown in Fig. 10.

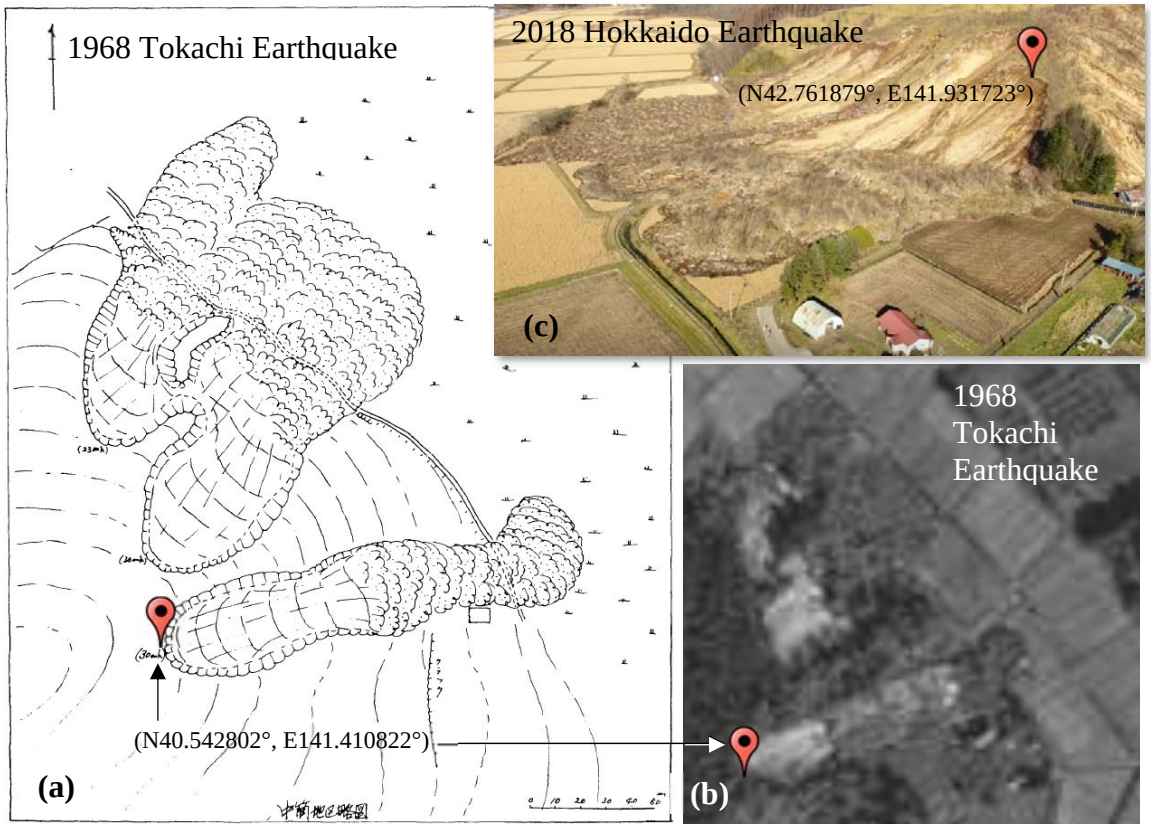

Fig. 9 – (a) Illustration in Reference [9] and (b) aerial photo (TO6810Y [10]) of triple landslides at Nakazutsu, Gonohe Town, Aomori (1968 Tokachi Earthquake). These landslides have a striking resemblance to (c) those in Atsuma Town, Hokkaido (2018 Hokkaido Earthquake).

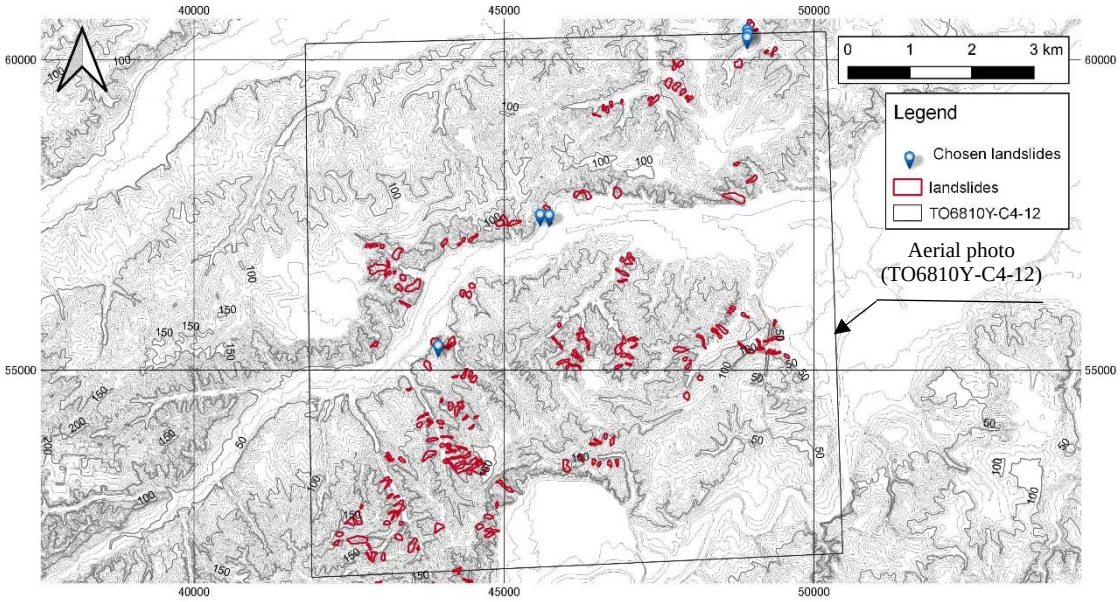

Fig. 10 – Photo-interpleted locations of landslides in the multiple landslide area west of Hachinohe City.
A slightly inclined parallelogram in the middle of the map is the area covered by a 1 to 40,000 scale aerial photo, TO6810Y, taken on Oct. 5, 1968 from an altitude of 6,000 feet by the Geospatial Information Authority of Japan [10].

Table 2 – Dimensions of 6 landslide masses shown in Fig. 10 with blue placemarks

Place	Latitude (deg.)	Longitude (deg.)	H_1 (m)	H_2 (m)	$H=H_1+H_2$ (m)	X_1 (m)	X_2 (m)	Observed X_1+X_2 (m)	Estimated X_1+X_2 (m)
Toyomanai	40.498328	141.35166	25	0	25	64	50	114	104.56
Nakazutsu 1	40.543854	141.41089	23	0	23	71	62	133	102.74
Nakazutsu 2	40.543356	141.41098	30	0	30	101	53	154	138.54
Nakazutsu 3	40.542802	141.41082	30	0	30	141	35	176	160.14
Kaminarasaki 1	40.517267	141.37122	55	5	60	177	100	277	263.58
Kaminarasaki 2	40.517182	141.37293	33.2	7	40.2	83	87	170	157.38

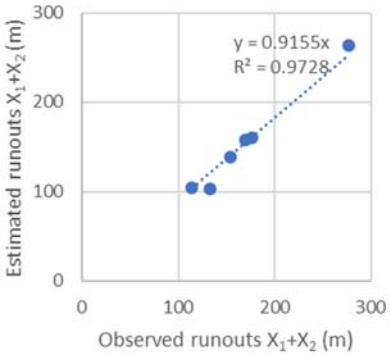

Fig. 11 – Comparison of the observed and estimated runouts $X_1 + X_2$ values.

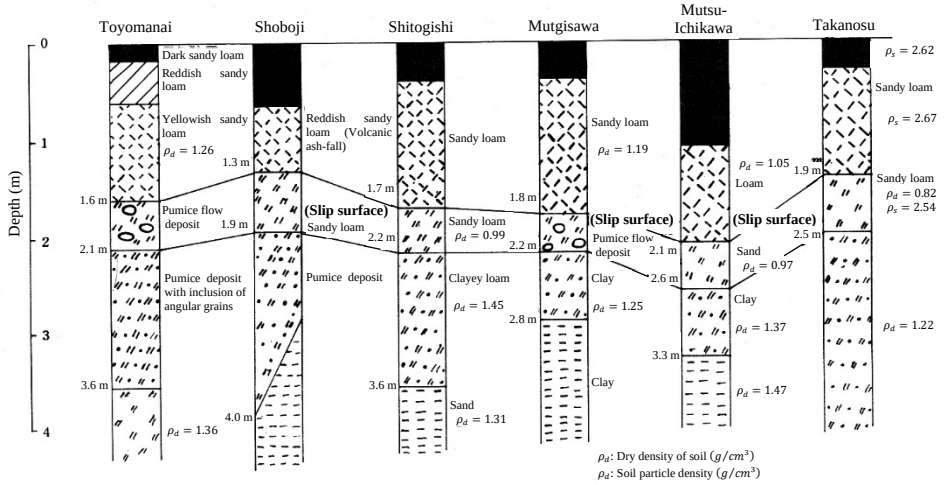

Fig. 12 – Soil profiles at 6 landslide locations [8]

4. Conclusions

The noteworthy common features of almost all landslides in the epicentral area of the 2018 Hokkaido Eastern Iburi Earthquake are that (1) root systems that can help trees "grab onto" soil and keep it clumped together hardly penetrated through the pumice/ volcanic ash drape and stayed above the slip surfaces, and that (2) almost a whole body of each landslide mass deposited over a flat land with little fraction of the mass remaining on the slope. Given these common features, dimensions of landslide masses that have deposited over flat rice fields have been examined. A multiple linear regression analysis for the relationship among the measured dimensions of total 30 landslide masses have given us both the average values of mobilized frictional coefficients $\mu_1 = 0.165$ on the slip surfaces and $\mu_2 = 0.36$ on the flat rice fields. However, the value of μ_1 for a smaller and gentler slope, which might have been wetter than the others, could have been even smaller than this value.

The observed geometric features of these landslide masses have a striking resemblance to those on hill slopes of Hachinohe area hit by the 1967 Tokachi Earthquake of M_w8.3, where the eruption of Mt. Towada about 13,000 years ago is believed to have left layers of volcanic material such as pumice draping the hilly landscape. The examined relation among slope dimensions such as height of slope H, original slope projection on a horizontal plane X_1, and runout distance $X_1 + X_2$ was found similar to the one derived from the multiple landslides in the 2018 Hokkaido Earthquake.

In the light of the fact that no small number of communities spread along bases of hills, further in-depth studies of landslide runout distances will be necessary to take necessary measures in a rational manner.

5. Acknowledgement

The authors have jointly conducted this field survey with the team of lifeline earthquake engineering experts of the American Society of Civil Engineers (ASCE) led by Mr. John Eidinger and Mr. Alex Tang. The authors are indebted to Mr. Masataka Shiga, PhD candidate at the University of Tokyo, who have joined the field survey and helped the authors flying a UAV to collect 3D images of terrains. The authors would like to express their sincere thanks to Dr. Yukihiro Tsukada, Executive Director of the Japan Society of Civil Engineers (JSCE hereafter), Dr. Takanobu Suzuki, Chairman, Dr. Yoshihisa Maruyama, Secretary General and all members of the Subcommittee of Lifeline Earthquake Engineering, JSCE Committee of Earthquake Engineering, Mr. Satoshi Suenaga, Kubota Corp., and Mr. Jiro Nakamura, Chubu Electric Power Co., Inc., for their generous supports to this joint survey. The authors' field survey was partially supported by the Grant-in-Aid for Scientific Research (A), No. 16H02744.

6. References

[1] Konagai K., Nakata A. M. (2019): Runouts of landslide masses detached in the 2018 Hokkaido Eastern Iburi Earthquake. *JSCE Journal of Disaster Fact-Sheets*, **FS2019-E-0001**, 1-6. Retrieved from http://committees.jsce.or.jp/disaster/FS2019-E-0001

[2] Konagai K., Nishiyama S., Ohishi K., Kodama D., Nanno Y. (2018): Large ground deformations caused by the 2018 Hokkaido Eastern Iburi Earthquake. *JSCE Journal of Disaster Fact-Sheets*, **FS2018-E-0003**, 1-8. Retrieved from http://committees.jsce.or.jp/disaster/FS2018-E-0003

[3] Geographical Information Authority of Japan (2018): *Landslide map on GeoJSON format for the epicentral area of the 2018 Hokkaido Eastern Iburi Earthquake*. (in Japanese). Retrieved from http://www.gsi.go.jp/common/000204728.zip

[4] Fire and Disaster Management Agency (2018): *The 31st disaster report of the 2018 Hokkaido Eastern Iburi Earthquake, Sept. 19, 2018, and actions that FDMA has taken so far*. (in Japanese). Retrieved from http://www.fdma.go.jp/bn/2018/detail/1074.html

[5] Geological Survey of Japan, AIST (2018). *Characteristics of pyroclastic deposit from Shikotsu quaternary eruptions*. (in Japanese). Retrieved from http://www.fdma.go.jp/bn/2018/detail/1074.html

[6] Weather record retrieving site, Japan Meteorological Agency, (in Japanese). Retrieved from https://www.data.jma.go.jp/obd/stats/etrn/index.php

[7] Aomori Prefecture (1969): *General report of damage in Aomori Prefecture caused by the 1968 Tokachi Earthquake*. Kyodo. (in Japanese).

[8] Kawakami F., Asada A., Yanagisawa E., Mori Y. (1969) *Report on the Tokachi-Oki Earthquake of 1968*, Department of Civil Engineering, Tohoku University. (in Japanese).

[9] Contributions from the Institute of Geology and Paleontology Tohoku University (1969): *Phenomena and disasters associated with earthquakes – Examples from the Tokachi-oki Earthquake of 1968 in eastern Aomori Prefecture*, **67**, p. 1-99. Retrieved from https://tohoku.repo.nii.ac.jp/?action=pages_view_main&active_action=repository_view_main_item_detail&item_id=118275&item_no=1&page_id=33&block_id=38

[10] Aerial photos retrieving site, Geographical Information Authority of Japan, (in Japanese). Retrieved from https://mapps.gsi.go.jp/maplibSearch.do#1

